Quantum Beats of the Radical Pair State in Photosynthetic Models Observed by Transient Electron Paramagnetic Resonance

ARTICLE *in* THE JOURNAL OF PHYSICAL CHEMISTRY · MARCH 1995

Impact Factor: 2.78 · DOI: 10.1021/j100012a064

8 AUTHORS, INCLUDING:

Gerd Kothe
University of Freiburg
140 PUBLICATIONS **2,458** CITATIONS
SEE PROFILE

Alexander Angerhofer
University of Florida
111 PUBLICATIONS **1,821** CITATIONS
SEE PROFILE

James R Norris
University of Chicago
240 PUBLICATIONS **7,897** CITATIONS
SEE PROFILE

Quantum Beats of the Radical Pair State in Photosynthetic Models Observed by Transient Electron Paramagnetic Resonance

Karl Laukenmann, Stefan Weber, and Gerd Kothe*

Institut für Physikalische Chemie, Universität Stuttgart, Pfaffenwaldring 55, D-70550 Stuttgart, Germany

Claudia Oesterle and Alexander Angerhofer†

3. Physikalisches Institut, Universität Stuttgart, Pfaffenwaldring 57, D-70550 Stuttgart, Germany

Michael R. Wasielewski, Walter A. Svec, and James R. Norris‡

Chemistry Division, Argonne National Laboratory, 9700 S. Cass Ave., Argonne, Illinois 60439

Received: August 22, 1994; In Final Form: January 3, 1995®

Time-resolved electron paramagnetic resonance (EPR) is used to study the transient spin polarization behavior of the light-induced radical pair state in the photosynthetic model system 2-tetraalkylphenylenediamine−Zn porphyrin−2-naphthoquinone. The time evolution of the transverse magnetization is monitored at various static magnetic fields. This implies a two-dimensional variation of the signal intensity with respect to both the magnetic field and time axis. Zero quantum coherence between two of the four eigenstates of the radical pair is observed at early times after the laser pulse. The beat frequencies vary significantly with the static magnetic field and extend up to 70 MHz. This model system is the first example where quantum beats have been observed of a correlated radical pair with protonated constituents.

Introduction

The elucidation of the photoinduced multistep charge separation in bacterial photosynthetic reaction centers (RC) in terms of structure,[1] energetics,[2,3] and dynamics[4-7] has spurred large efforts to mimic it by the design of artificial model systems. Recent reviews of this vastly expanding field can be found elsewhere.[8,9]

By careful adjustment of the redox properties of the reacting partners, supermolecules were designed that feature a high quantum yield of light-induced charge separation in the solid state as well as long lifetimes of the resulting radical pair states.[10-12] Recently, a photosynthetic model was reported consisting of a zinc porphyrin primary electron donor (ZnP), covalently linked to a naphthoquinone electron acceptor (NQ), and an *N,N,N',N'*-tetraalkyl-*p*-phenylenediamine secondary electron donor (TAPD)[13] (see Figure 1a). This molecule can be prepared in four different isomers, depending on the linkage of the TAPD and NQ entities to the phenyl rings of the Zn porphyrin. In this contribution we report transient EPR studies performed on what is termed the 2−2 isomer (or 2-TAPD−ZnP−2-NQ[14]). At low temperatures in solid organic glasses this molecule stores 1.85 eV of energy for about 4 ms in its radical pair state $TAPD^+-ZnP-NQ^-$ with a quantum yield of 67%[13,14] (see kinetic scheme in Figure 1b). The model compound exhibits a characteristic light-induced spin-polarized EPR signal.[13,14]

Electron spin polarization due to a correlated radical pair was first detected as an "out-of-phase" electron spin echo signal in photosynthetic algae.[15,16] Subsequently, corresponding EPR signals have been observed in the course of photochemical reactions in viscous solutions,[17] in micellar systems,[18,19] in cyclodextrin cavities,[20] in photochemically produced biradicals in liquid solution,[21,22] on surfaces[23] as well as in photosynthetic reaction centers,[24,25] and in photosynthetic model systems.[26,27]

The observation of spin-polarized radical pairs requires two conditions to be met:[17,19] First, the two radical species forming the pair should experience an appreciable exchange and/or dipolar interaction since it determines the splitting between the antiphase EPR lines characteristic for the radical pair spin polarization. Second, the spin−spin relaxation time T_2 should be long compared to the time needed for the observation of the EPR signal. Modern instruments feature time resolutions of the order of 10 ns, and in the case of pulsed microwave setups (i.e., spin-echo or Fourier transform (FT) spectrometers) dead times of the order of 60 ns, allowing the observation of short-lived coupled radical pairs.

Ignoring hyperfine interactions, the EPR spectrum of a spin-correlated radical pair consists of four lines arranged in two doublets, centered at the g values of the individual radicals.[17,19] Under solid-state conditions the total EPR line shape is a superposition of the four-line spectra for all different orientations with respect to the external magnetic field. The splitting within a doublet is determined by the exchange and dipolar contributions to the spin-spin interaction. The intensity and sign of these EPR lines depends on the spin multiplicity of the precursor states. In many cases the radical pair is created in a virtually pure singlet state, yielding an e/a (low-field emissive/high-field absorptive) polarization for both doublets. An instructive vector diagram method taking into account both the correlated radical pair polarization and conventional chemically induced electron polarization (CIDEP) has been published by Norris et al.[28]

Coherent time domain oscillations of the spin polarization pattern naturally emerge from the correlated radical pair concept. Recently, such quantum beats have been predicted in the transverse magnetization of radical pairs in photosynthetic RCs.[29,30] Additional theoretical examinations of these transient

* To whom correspondence should be addressed. Present address: Institut für Physikalische Chemie, Universität Freiburg, Albertstr. 21, D-79104 Freiburg.

† Present address: Chemistry Department, The University of Florida, Gainesville, FL 32611.

‡ And Chemistry Department, The University of Chicago, Chicago, IL 60637.

® Abstract published in *Advance ACS Abstracts,* March 1, 1995.

0022-3654/95/2099-4324$09.00/0

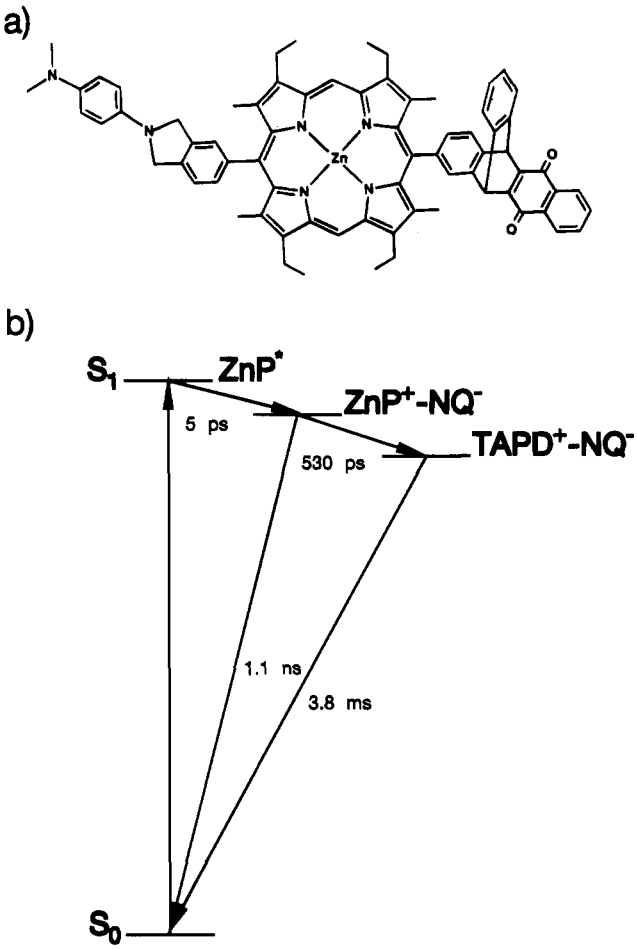

Figure 1. (a) Molecular structure of the photosynthetic model system 2-TAPD−ZnP−2-NQ. (b) Kinetic steps following a short initial exciting laser pulse and leading to the formation of the correlated radical pair $TAPD^+-NQ^-$.

phenomena have appeared subsequently.[31,32] Quantum beats in the radical pairs of photosynthetic RCs, i.e., fixed-distance radical pairs, have recently been reported by Kothe et al.[33−36] and Bittl et al.[37] Generally, observation of quantum beats in these highly complex systems was only possible if the following conditions were met:

1. High time resolution of ≤10 ns using direct detected EPR with no limitations due to intrumental dead time. In the case of plant photosystem I and iron-depleted bacterial RCs the beat frequencies reached up to 25 MHz.[33,35]

2. In order to avoid destructive averaging of coherent oscillations narrow band microwave excitation is required for powder samples, where anisotropic magnetic interactions dominate.

3. Because of hyperfine interactions, rapid damping of quantum beat oscillations occurs. Thus the use of fully deuterated samples appeared to be mandatory for the observation of quantum beats.

In this contribution we report the first observation of quantum beats in the radical pair state of a photosynthetic model system, i.e., 2-TAPD−ZnP−2-NQ (see Figure 1a). Earlier reports of oscillations of the spin polarization with rather long oscillation periods observed with FT-EPR[38] could not be substantiated in this work. The present experiments were carried out on fully protonated samples with fairly large hyperfine interactions, particularly in the TAPD part. Apparently, strong hyperfine interactions do not necessarily totally average the quantum beat oscillations.

Materials and Methods

The synthesis of the 2-TAPD−ZnP−2-NQ model system has been described earlier.[13] The material was kept in the dark at −20 °C as a dark red powder. Samples for the EPR experiments were always prepared freshly from this stock material as follows: First, the material was thoroughly purified under nitrogen atmosphere using thin layer chromatography (TLC). The eluting solvent was 95%/5% dichloromethane/acetone. The uppermost band shows a cherry-red color containing the purified compound. It was scraped off the TLC plate, the compound was extracted from the silica gel with acetone, and immediately filtered to remove the silica gel which acts as a catalyst and decomposes the molecule under illumination in the presence of oxygen, and the acetone was evaporated using a stream of dry nitrogen gas. The pure material was then dissolved in ultrapure MTHF (Aldrich, distilled and stored over potassium/sodium alloy), and the solution was filled in an EPR quartz tube of 2 mm inner diameter. After several freeze−pump−thaw cycles the sample tube was sealed under vacuum. Sample temperature was controlled by a helium flow cryostat (Oxford CF-935) and was stable to within ±0.1 K.

The setup for the transient EPR experiment was the same as described earlier.[34,35] For optical excitation the frequency-doubled output of the Nd:YAG laser was used. With the short-pulse option we obtained 2.5 ns pulse widths and 300 mJ/pulse output. For the actual experiment the intensity was attenuated to approximately 10 mJ/pulse. The repetition rate of the laser was 10 Hz.

Theoretical Background

The theory on which our analysis is based has been outlined before.[30,33−36] Here, we summarize the main features and introduce the model parameters used in the Discussion section.

The total spin Hamiltonian, $H(\Omega,t)$, depends on the orientation, Ω, of the radical pair and can be divided into five parts:

The first term, describing the Zeeman interactions of the electron spins $\boldsymbol{S}_i$, $i = 1, 2$, with the static magnetic field $\boldsymbol{B}_0 = (0, 0, B_0)$ is given by

$$H_Z(\Omega) = \beta \boldsymbol{B}_0 \cdot [\mathbf{g}_1(\Omega) \cdot \boldsymbol{S}_1 + \mathbf{g}_2(\Omega) \cdot \boldsymbol{S}_2] \quad (1)$$

where β and $\mathbf{g}_i$ ($i = 1, 2$) are the Bohr magneton and the $\mathbf{g}$ tensor of radical i, respectively. In the presence of the rotating microwave field $\boldsymbol{B}_1 = (B_1 \cos(\omega t), B_1 \sin(\omega t), 0)$ the Hamiltonian includes the radication term

$$H_R(\Omega,t) = \beta \mathbf{B}_1 \cdot [\mathbf{g}_1(\Omega) \cdot \boldsymbol{S}_1 + \mathbf{g}_2(\Omega) \cdot \boldsymbol{S}_2] \quad (2)$$

where $\boldsymbol{B}_1$ denotes the magnitude of the microwave field.

The next two terms of the total spin Hamiltonian account for the isotropic and anisotropic spin−spin coupling of the radical pair

$$H_{Ex} = J(Q_T - Q_S) \quad (3)$$

$$H_D(\Omega) = (\boldsymbol{S}_1 + \boldsymbol{S}_2) \cdot \mathbf{D}(\Omega) \cdot (\boldsymbol{S}_1 + \boldsymbol{S}_2) \quad (4)$$

where

$$Q_T = ({}^3/_4 + \boldsymbol{S}_1 \cdot \boldsymbol{S}_2) \quad (5)$$

$$Q_S = ({}^1/_4 - \boldsymbol{S}_1 \cdot \boldsymbol{S}_2) \quad (6)$$

and J and $\mathbf{D}(\Omega)$ are the electron exchange interaction and dipolar coupling tensor, respectively. Since $\mathbf{D}(\Omega)$ is traceless, two parameters, D and E, completely determine the diagonal tensor.

The fifth term of the total spin Hamiltonian describes the nuclear hyperfine interactions in the approximation for a weakly coupled radical pair,

$$H_{\mathrm{HFI}}(\Omega) = \sum_k \boldsymbol{I}_{1k}\cdot\mathbf{A}_{1k}(\Omega)\cdot\boldsymbol{S}_1 + \sum_l \boldsymbol{I}_{2l}\cdot\mathbf{A}_{2l}(\Omega)\cdot\boldsymbol{S}_2 \qquad (7)$$

where $\boldsymbol{I}_{ik}$ is the spin operator of nucleus k in radical i ($i = 1, 2$) and $\mathbf{A}_{ik}$ is the corresponding hyperfine tensor. a_{ik} denotes the isotropic hyperfine coupling constant,

$$a_{ik} = {}^1/_3(A_{ik}^X + A_{ik}^Y + A_{ik}^Z) \qquad (8)$$

and A_{ik}^j ($j = X, Y, Z$) are the principal values of $\mathbf{A}_{ik}$, respectively.

At present, nuclear quadrupole interactions have been neglected, since information about the ^{14}N quadrupole tensors is lacking for the TAPD$^+$ moiety. However, a more rigorous analysis of the experimental data, including possible nuclear modulations, requires consideration of these interactions, as in the case of plant photosystem I.[36]

We now take the initial state of the radical pair to be pure singlet which is the case in the photosynthetic model and assume that it is created instantaneously by a negligibly short light pulse. As shown previously,[33-37] such a radical pair is formed with spin-correlated populations of two of the four electron spin levels and zero quantum coherence between these states. In the absence of a microwave field, the eigenstate populations are constant in time while the zero quantum coherence oscillates at a frequency

$$\nu_{\mathrm{ZQC}} = (1/h)\{[2J + 2/3D^{zz}(\Omega)]^2 + [(g_1^{zz}(\Omega) - g_2^{zz}(\Omega))\beta B_0 + \sum_k A_{1k}^{zz}(\Omega)M_{1k}^i - \sum_l A_{2l}^{zz}(\Omega)M_{2l}^j]^2\}^{(1/2)} \qquad (9)$$

where

$$M_{1k}^i = I_{1k}, I_{1k} - 1, ..., -I_{1k} \qquad (10)$$

$$M_{2l}^j = I_{2l}, I_{2l} - 1, ..., -I_{2l} \qquad (11)$$

and z denotes the direction of the static magnetic field.

The application of a continuous microwave field has two effects. First, it converts longitudinal magnetization associated with the population difference between neighboring states in transverse magnetization. This gives the Torrey oscillations

$$\nu_{\mathrm{TO}} \approx (1/2h)(g_1 + g_2)\beta B_1 \qquad (12)$$

virtually independent of B_0 but linearly dependent on B_1. Second, it converts zero quantum coherence into observable single quantum coherence, significantly varying with B_0. Because of hyperfine interactions, rapid averaging of these oscillations is expected even in the case of narrow band microwave excitation. Thus, the manifestation of zero quantum coherence is likely to be observed only shortly after the laser pulse.

Results

Fully protonated samples of the photosynthetic model 2-TAPD−ZnP−2-NQ where irradiated at 30 K with the frequency doubled output of the Nd:YAG laser with pulses of 10 mJ energy and 2.5 ns pulse width. The time evolution of the transverse magnetization was monitored for various static magnetic fields. The complete experimental data set is shown in Figure 2. It consists of transient signals taken with a sample

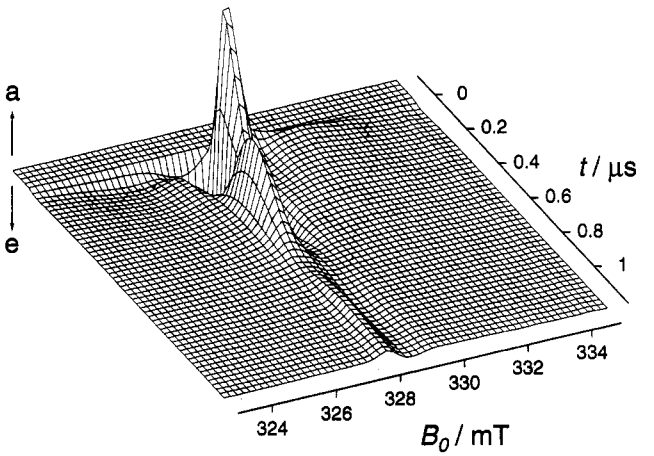

Figure 2. Complete data set of the transient EPR signal of the light-induced radical pair of 2-TAPD−ZnP−2-NQ. Positive signals indicate enhanced absorptive (a), negative signals emissive (e) polarization. Experimental parameters: temperature 30 K, microwave frequency $\omega/2\pi$ = 9.2095 GHz, microwave power B_1 = 0.046 mT.

resolution of 5 ns per data point as determined by the transient digitizer at equidistant magnetic field positions covering the whole spectrum. This implies a two-dimensional variation of the signal intensity with respect to both the magnetic field and the time axis. The microwave frequency was 9.2095 GHz, and the microwave power was 200 mW which corresponds to a B_1 of 0.046 mT. Positive signals indicate absorptive (a) and negative emissive (e) spin polarization. Transient spectra can be extracted from this data set at any fixed time after the laser pulse as slices parallel to the magnetic field axis. Likewise, the time evolution of the transverse magnetization may be obtained for any given field as a slice along the time axis. Transient spectra taken at 20, 50, 70, and 130 ns after the laser pulse with a time window of 5 ns (one data point of the transient digitizer) are shown in Figure 3. At very early times (≤20 ns) the spectrum is much broader than at later times. A detailed analysis reveals that lifetime broadening actually dominates the early spectra.[34] At later times (i.e., 70 ns) the spin-polarized transient spectrum reveals a strong doublet signal with a low-field emissive maximum at 327.89 mT (g = 2.0068) and a high-field absorptive maximum at 328.53 mT (g = 2.0029). Superimposed is a broad EPR signal which extends over 8 mT (see amplified wings of the spectrum at 130 ns). The low-field part of this signal is emissive peaking at 326.16 mT (g = 2.0174), whereas the high-field part is absorptive with a maximum at 331.07 mT (g = 1.9875). The strong doublet signal has been observed before by FT-EPR at early times after the laser pulse and was assigned to the spin-polarized signal of the naphthoquinone part of the radical pair.[38] The broad wings were not detected by pulsed EPR, possibly because of the nonzero dead time in the microwave detection path of the pulsed experiment. However, they appear in the quasi continuous wave light-modulated EPR experiment.[14]

Figure 4 depicts the time evolution of the transverse magnetization, measured at seven selected field positions (A−G, same as in Figure 3). Apparently, all transients exhibit fast oscillations at early times after the laser pulse (see left column of Figure 4). Note that the frequency of these oscillations varies significantly across the spectrum, indicating the anisotropic nature of these transients. Generally, the modulation depth is rather weak, requiring high sensitivity of the experimental setup. Only at the zero crossing points of the spectrum (field positions B, D, and F) the oscillations dominate the short time evolution of the transverse magnetization. For convenience all time profiles have been normalized to equal height. Note the very

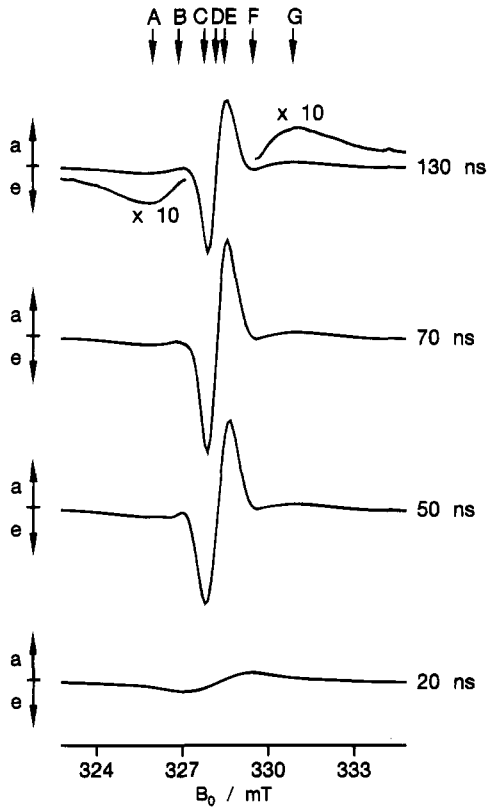

Figure 3. Transient EPR lineshapes of the light-induced radical pair $TAPD^+-NQ^-$ at various times after the initial laser pulse. Signal sign convention and experimental parameters are as in Figure 2. Various field positions are marked from A to G. The development of the spin-polarized EPR signal in time at these field positions is shown in Figure 4.

fast oscillations at field positions A and G with frequencies of about 50 MHz, which nicely demonstrate the high time resolution of our experimental setup. In fact, oscillation frequencies of up to 70 MHz were picked up at the high- and low-field ends of the spectrum.

Interestingly, the slow persisting oscillations (see right column of Figure 4) cannot all be assigned to Torrey precessions with a frequency of $\nu_{TO} \approx 1.3$ MHz. Rather, there are additional modulations of the transverse magnetization whose frequencies are largely independent of B_1 (data not shown). Possibly, these additional coherences represent nuclear quantum beats associated with the nonadiabatic change of the spin Hamiltonian at the instant of the laser pulse.[36,37] A detailed analysis of this interesting phenomenon is deferred to a later publication.

The existence of zero quantum precessions is clearly visible from a contour plot representation of the two-dimensional EPR experiment. Figure 5 shows the Fourier transform of the time profiles as a function of B_0. The modulus of the complex Fourier transform is plotted with contour lines at constant intensity in steps of 4% of the maximum intensity. Basically, two contributions can be distinguished in the ω_2 domain: isotropic Torrey oscillations in the range of 1−2 MHz, possibly together with nuclear quantum beats, and anisotropic zero quantum precessions with frequencies up to 60 MHz.

The overall shape of the contour plot corresponds to that observed for the secondary radical pair in plant photosystem I.[34] In the latter case the pronounced variation of the precession frequencies across the powder spectrum has been used to evaluate the geometry of the underlying radical pair. Apparently, the analysis of zero quantum precessions as a function of the external field can provide detailed information on the spatial arrangement of the radicals in a spin-correlated radical pair.

Discussion

A full theoretical analysis of the spin-polarized spectrum as well as the quantum beat oscillations requires knowledge of the **g** tensors in $TAPD^+-NQ^-$, the exchange interaction, the dipolar interaction, the relevant hyperfine interactions, and the relative orientations of the various magnetic tensors. Only part of this information is available at present:

1. The **g** tensor of NQ^- and its orientation within the molecular frame are known from W-band EPR studies.[39] They are $g^X_{NQ} = 2.005\,79$, $g^Y_{NQ} = 2.005\,05$, and $g^Z_{NQ} = 2.002\,29$.

2. The **g** tensor of the $TAPD^+$ is not known. However, the **g**-tensor components of a similar molecule, Wurster's blue, have been determined as $g^X = 2.003\,25$, $g^Y = 2.003\,25$, and $g^Z = 2.002\,80$.[40]

3. The zero-field splitting parameters D and E are estimated on the basis of a center-to-center distance between the radicals of 23 Å.[41] The corresponding values amount to $D \approx -0.23$ mT and $E = 0$. For the exchange interaction parameter a small value of $J = 0.05$ mT has been assumed.

4. The hyperfine interactions of $TAPD^+$ are not known in any great detail. Data obtained for Wurster's blue indicate that the spin density is high not only at the two nitrogens with $A^X_N = 0.30$ mT, $A^Y_N = 0.30$ mT, $A^Z_N = 1.51$ mT, but also on the 10 methyl protons $A^X_H = 0.71$ mT, $A^Y_H = 0.71$ mT, $A^Z_H = 0.63$ mT.[42] Wurster's blue actually has 12 methyl protons. In our case two of them have been removed and substituted by the bonds to the phenyl ring of the ZnP. The large methyl proton hyperfine interactions are basically the reason for the unusually broad doublet spectrum underlying the NQ^- doublet. It supports the earlier identification of NQ^- being responsible for the narrow doublet signal.[38]

5. The hyperfine interactions of NQ^- have been evaluated.[39,42] Here we consider four equivalent protons with $A^X_{H(NQ)} = 0.23$ mT, $A^Y_{H(NQ)} = 0.33$ mT, and $A^Z_{H(NQ)} = 0.21$ mT.

6. The orientations of the various magnetic tensors may in principle be obtained from the geometry of the photosynthetic model system which is known from the characterization of the structures of all intermediates in the synthesis by NMR (with some uncertainties regarding the state of conformation of the two phenyl rings). For simplicity we assume that the hyperfine tensors in $TAPD^+$ and NQ^- are collinear with the corresponding **g** tensors. The Euler angles, relating the respective magnetic tensor and the molecular frame of reference (**g** tensor of NQ^- [43]), are thus assumed to be $\Theta_D = 30°$, $\Psi_D = 30°$ (dipolar tensor), and $\Theta_{TAPD} = 70°$, $\Psi_{TAPD} = 0°$ (**g** tensor of $TAPD^+$).

7. The relaxation times $T_1 = 700$ ns (at 30 K) and $T_2 = 390$ ns (at 6 K) of $TAPD^+-ZnP-NQ^-$ have been determined by transient and pulsed EPR.[44] It was found that T_2 varies between 340 ns and 440 ns, depending on the field position.

Model calculations have been performed employing the parameters discussed above. Generally, the agreement between observed and calculated contour plots is satisfactory. In particular, the frequencies of the coherent oscillations and their dependence on the static magnetic field is satisfactorily reproduced by the calculations. We therefore conclude that quantum beat oscillations have been detected in a photosynthetic model system. This result confirms the assignment of the broad wings in the transient spectrum (see Figure 3) to $TAPD^+$ from $TAPD^+-NQ^-$. Moreover, it explains the unusual high frequencies of the quantum beats observed for this system. Because of the large hyperfine interactions in $TAPD^+$, the beat frequen-

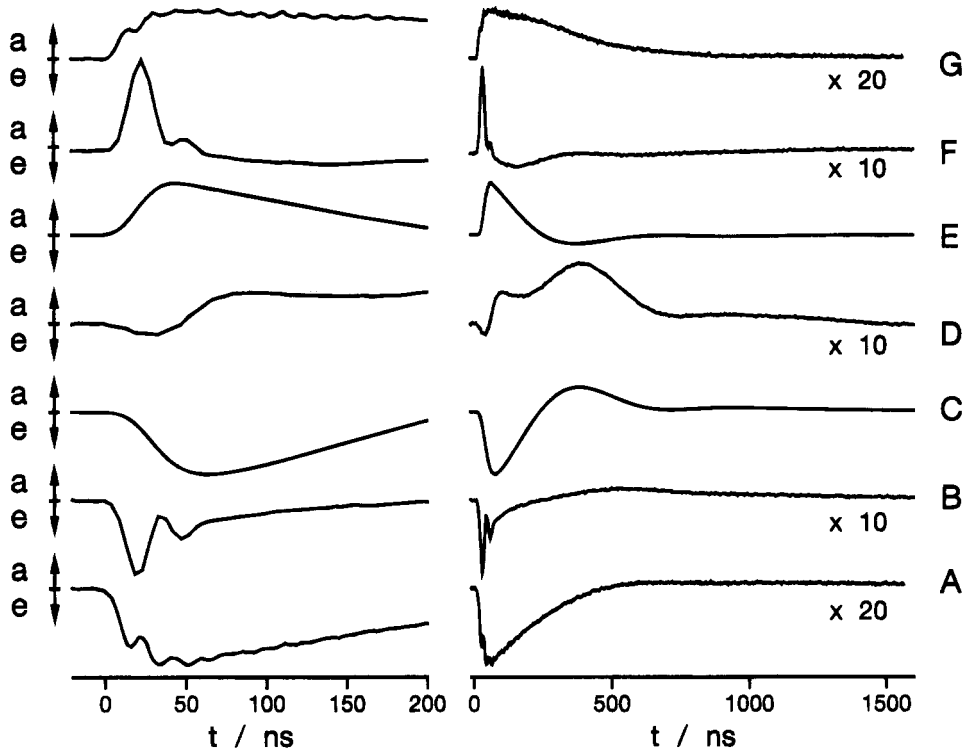

Figure 4. Time development of the transient EPR signal of the light-induced radical pair $TAPD^+-NQ^-$ at various field positions (A through G) indicated in Figure 3. Signal sign convention and experimental parameters are as in Figure 2. For the traces on the left the time axis has been expanded to show the behavior at early times after the laser pulse. The time profiles have been normalized to approximately the same height with the respective amplification factors indicated.

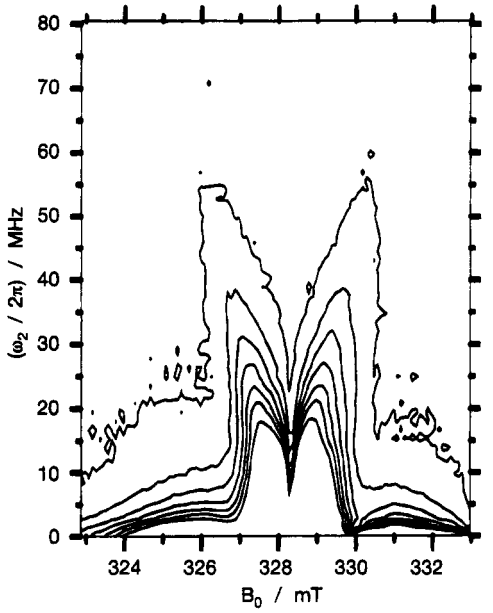

Figure 5. Contour plot of the Fourier transformation in time ($t \rightarrow \omega_2$) of the two-dimensional data set of Figure 2. Contour lines have been plotted in steps of 4% of the maximum intensity. Only the data between 0.2 and 24.2% are shown to emphasize the quantum beat part of the oscillations which extends to more than 60 MHz in ω_2.

cies considerably exceed those expected from the **g**-tensor difference in $TAPD^+$ and NQ^-.

Not surprisingly, however, there are deviations between the calculated time profiles and their experimental counterparts. They arise from uncertainties in the various structural and magnetic parameters, for which accurate values do not exist. The molecular structure of 2-TAPD−ZnP−2-NQ as determined by NMR spectroscopy[13] supports a highly rigid structure in which the orientation and distance between TAPD and NQ are restricted to a relatively narrow distribution of conformations. The methyl groups of the ZnP strongly restrict the rotation of the adjacent *meso*-phenyl groups that hold both TAPD and NQ. This results in two diastereomers in which both the orientation and distance between TAPD and NQ are slightly different. In addition, the angular distributions due to torsional motions of the phenyl groups within their respective potential wells is not known in detail. A simultaneous fit of the B_0-dependent time profiles could provide the necessary information.

Studies along these lines, using deuterated 2-TAPD−ZnP−2-NQ, are currently in progress. Detailed structural information is to be expected from such studies,[34] which will be essential for the understanding of the charge separation in this model system and, by comparison, will assist our understanding of the primary events in natural photosynthesis. Here we want to stress the following points:

1. For the first time a protonated system was shown to exhibit the quantum beat phenomenon. Previously it has only been observed in fully deuterated samples since the broad distribution of resonance frequencies in a hyperfine-broadened system dampens out the coherences. In our system we have to deal with large hyperfine interactions, at least one order of magnitude larger than in the natural photosynthetic preparations where quantum beats have been observed so far. In fact, the large hyperfine interaction may be advantageous for the observation of qunatum beats since the spectrum is much more spread out and better resolved in ω_2, the zero quantum frequency axis.

2. The quantum beats in the photosynthetic model system are hyperfine-driven. Inspection of eq 9 reveals that the zero quantum coherence frequency is dominated by the hyperfine term in contrast to comparable cases in plant and bacterial reaction centers. This dominance results from the relatively weak exchange and dipolar interactions in the $TAPD^+-NQ^-$ radical pair.

3. Possibly, nuclear quantum beats have been observed in the photosynthetic model system. Since the initial nuclear spin configurations are not eigenstates of the radical pair Hamiltonian, the light pulse creates a coherent time evolution of the nuclear spin system, which could manifest itself as nuclear modulation patterns in the transverse electron magnetization.

Conclusions

We have for the first time demonstrated the existence of zero quantum coherences in a protonated system and a photosynthetic model compound, 2-TAPD−ZnP−2-NQ, using fast transient EPR. Furthermore, we succeeded in monitoring the full spin-polarized spectrum including the broad $TAPD^+$ lines. The spectrum as well as the quantum beats indicate that the photosynthetic model system forms a correlated radical pair upon light excitation, similar to the reaction centers of photosynthetic bacteria and plant photosystem I. In this respect, 2-TAPD−ZnP−2-NQ proves to be a rather good model of the photosynthetic reaction center, even though its molecular constituents are quite distinct from the natural ones.

Acknowledgment. This research was financially supported by the Deutsche Forschungsgemeinschaft. Research at ANL was supported by the Divisions of Chemical Sciences, Office of Basic Energy Sciences, U.S. Department of Energy, under contract W-31-109-Eng-38. J.R.N. gratefully acknowledges support from the Alexander von Humboldt foundation. A.A. and M.R.W. acknowledge support from NATO under CRG.900982.

References and Notes

(1) Deisenhofer, J.; Epp, O.; Miki, K.; Huber, R.; Michel, H. *J. Mol. Biol.* **1984**, *180*, 385.
(2) Goldstein, R. A.; Takiff, L.; Boxer, S. G. *Biochim. Biophys. Acta* **1988**, *934*, 235.
(3) Takiff, L.; Boxer, S. G. *Biochim. Biophys. Acta* **1988**, *932*, 325.
(4) Rockley, M. G.; Windsor, M. W.; Cogdell, R. J.; Parson, W. W. *Proc. Natl. Acad. Sci. U.S.A.* **1975**, *72*, 2251.
(5) Kirmaier, C.; Holten, D.; Parson, W. W. *Biochim. Biophys. Acta* **1985**, *810*, 49.
(6) Holzapfel, W.; Finkele, U.; Kaiser, W.; Oesterhelt, D.; Scheer, H.; Stilz, H. U.; Zinth, W. *Chem. Phys. Lett.* **1989**, *160*, 1.
(7) DiMagno, T. J.; Norris, J. R. In *The Photosynthetic Reaction Center*; Deisenhofer, J., Norris, J. R., Eds.; Academic Press: San Diego, CA, 1993; Vol. II, p 105.
(8) Gust, D.; Moore, T. A. In *The Photosynthetic Reaction Center*; Deisenhofer, J., Norris, J. R., Eds.; Academic Press: San Diego, CA, 1993; Vol. II, p 419.
(9) Wasielewski, M. R. In *The Photosynthetic Reaction Center*; Deisenhofer, J., Norris, J. R., Eds.; Academic Press: San Diego, CA, 1993; Vol. II, p 465.
(10) Wasielewski, M.R.; Johnson, D. G.; Svec, W. A.; Kersey, K. M.; Minsek, D. W. *J. Am. Chem. Soc.* **1988**, *110*, 7219.
(11) Gaines, III, G. L.; O'Neil, M. P.; Svec, W. A.; Niemczyk, M. P.; Wasielewski, M. R. *J. Am. Chem. Soc.* **1991**, *113*, 719.
(12) Wasielewski, M. R.; Gaines, III, G. L.; O'Neil, M. P.; Svec, W. A.; Niemczyk, M. P.; Prodi, L.; Gosztola, D. In *Dynamics and Mechanisms of Photoinduced Electron Transfer and Related Phenomena*; Mataga, N., Okada, T., Masahura, H., Eds.; Elsevier: Amsterdam, 1991; p 133.
(13) Wasielewski, M. R.; Gaines, III, G. L.; O'Neil, M. P.; Svec, W. A.; Niemczyk, M. P. *J. Am. Chem. Soc.* **1990**, *112*, 4559.
(14) Wasielewski, M. R.; Gaines, III, G. L.; O'Neil, M. P.; Niemczyk, M. P.; Svec, W. A. In *Supramolecular Chemistry*; Balzani, V., De Cola, L. Eds.; Kluwer Academic Publishers: Dordrecht, The Netherlands, 1992; p. 201.
(15) Thurnauer, M. C.; Norris, J. R. *Chem. Phys. Lett.* **1980**, *76*, 557.
(16) Thurnauer, M. C.; Rutherford, A. W.; Norris, J. R. *Biochim. Biophys. Acta* **1982**, *682*, 332.
(17) Buckley, C. D.; Hunter, D. A.; Hore, P. J.; McLauchlan, K. A. *Chem. Phys. Lett.* **1987**, *135*, 307.
(18) Sakaguchi, Y.; Hayashi, H.; Murai, H.; I'Haya, Y. J. *Chem. Phys. Lett.* **1984**, *110*, 275.
(19) Closs, G. L.; Forbes, M. D. E.; Norris, J. R. *J. Phys. Chem.* **1987**, *91*, 3592.
(20) Murai, H.; Yamamoto, Y.; I'Haya, Y. J. *Can. J. Chem.* **1991**, *69*, 1643.
(21) Maeda, K.; Terazima, M.; Azumi, T.; Tanimoto, Y. *J. Phys. Chem.* **1991**, *95*, 197.
(22) Closs, G. L.; Forbes, M. D. E. *J. Phys. Chem.* **1991**, *95*, 1924.
(23) Forbes, M. D. E.; Myers, T. L.; Dukes, K. E.; Maynard, H. D. *J. Am. Chem. Soc.* **1992**, *114*, 353.
(24) Hore, P. J.; Hunter, D. A.; McKie, C. D.; Hoff, A. J. *Chem. Phys. Lett.* **1987**, *137*, 495.
(25) Stehlik, D.; Bock, C. H.; Petersen, J. *J. Phys. Chem.* **1989**, *93*, 1612.
(26) Hasharoni, K.; Levanon, H.; Tang, J.; Bowman, M. K.; Norris, J. R.; Gust, D.; Moore, T. A.; Moore, A. L. *J. Am. Chem. Soc.* **1990**, *112*, 6477.
(27) Lendzian, F.; von Maltzan, B. *Chem. Phys. Lett.* **1991**, *180*, 191.
(28) Norris, J. R.; Morris, A. L.; Thurnauer, M. C.; Tang, J. *J. Chem. Phys.* **1990**, *92*, 4239.
(29) Salikhov, K. M.; Bock, C. H.; Stehlik, D. *Appl. Magn. Reson.* **1990**, *1*, 195.
(30) Bittl, R.; Kothe, G. *Chem. Phys. Lett.* **1991**, *177*, 547.
(31) Wang, Z.; Tang, J.; Norris, J. R. *J. Magn. Reson.* **1992**, *97*, 322.
(32) Zwanenburg, G.; Hore, P. J. *Chem. Phys. Lett.* **1993**, *203*, 65.
(33) Kothe, G.; Weber, S.; Bittl, R.; Ohmes, E.; Thurnauer, M. C.; Norris, J. R. *Chem. Phys. Lett.* **1991**, *186*, 474.
(34) Kothe, G.; Weber, S.; Ohmes, E.; Thurnauer, M. C. Norris, J. R. *J. Phys. Chem.* **1994**, *98*, 2706.
(35) Kothe, G.; Weber, S.; Ohmes, E.; Thurnauer, M. C.; Norris, J. R. *J. Am. Chem. Soc.* **1994**, *116*, 7229.
(36) Weber, S.; Ohmes, E.; Thurnauer, M. C.; Norris, J. R.; Kothe, G. *Proc. Natl. Acad. Sci. U.S.A.*, submitted, for publication (1994).
(37) Bittl, R.; van der Est, A.; Kamlowski, A.; Lubitz, W.; Stehlik, D. *Chem. Phys. Lett.* **1994**, *226*, 349.
(38) Angerhofer, A.; Wasielewski, M. R.; Gaines, III, G. L.; O'Neil, M. P.; Svec, W. A.; Niemczyk, M. P. *Z. Phys. Chem.* **1991**, *172*, 17.
(39) Burghaus, O.; Plato, M.; Rohrer, M.; Möbius, K. *J. Phys. Chem.* **1993**, *97*, 7639.
(40) Falle, H. R.; Luckhurst, G. R. *J. Magn. Reson.* **1970**, *3*, 161.
(41) Coffman, R. E.; Beuttner, G. R. *J. Phys. Chem.* **1979**, *83*, 2387.
(42) Kirste, B. *Magn. Reson. Chem.* **1987**, *25*, 166.
(43) Hales, B. F. *J. Am. Chem. Soc.* **1975**, *97*, 5993.
(44) Oesterle, C. Diploma thesis, Universität Stuttgart, 1993.

JP9422811